Digital Signal Processing 78 (2018) 20–29

Contents lists available at ScienceDirect

Digital Signal Processing

www.elsevier.com/locate/dsp

Inhomogeneous quadratic tests in transient signal detection: Closed-form upper bounds and application in GNSS ☆

Daniel Egea-Roca *, Gonzalo Seco-Granados, José A. López-Salcedo

Department of Telecommunication and Systems Engineering, IEEC-CERES, Universitat Autònoma de Barcelona (UAB), 08193 Bellaterra (Barcelona), Spain

ARTICLE INFO

Article history:
Available online 1 March 2018

Keywords:
Signal detection
Inhomogeneous quadratic test
Gaussian random
Edgeworth
Extreme Value Theory (EVT)

ABSTRACT

This paper focuses on transient signal detection based on inhomogeneous quadratic tests, which involve the sum of a dependent non-central chi-square with a Gaussian random variable. These tests arise in many signal processing-related problems in biomedicine, finance or engineering, where sudden changes in the magnitude under analysis need to be promptly detected. Unfortunately, no closed-form expression is available for the density of inhomogeneous quadratic tests, which poses some concerns and limitations in their practical implementation. In particular, when trying to assess their detection performance in terms of probability of detection and probability of false alarm. In order to circumvent this limitation, two closed-form approximations based on results from Edgeworth series expansions and Extreme Value Theory (EVT) are proposed in this work. The use of these approximations is shown through a specific case of study in the context of transient detection for signal quality monitoring in Global Navigation Satellite Systems (GNSS). Numerical results are provided to assess the goodness of the proposed approximations, and to highlight their interest in real life applications.

1. Introduction

Detecting the presence of an event is a recurrent task in many signal processing-related problems arising in biomedicine, finance or engineering, where decisions are taken based on the observation of the signal samples provided by some system. In particular, these samples are processed by a decision function whose outcome is compared to a predefined threshold for accepting or rejecting the hypothesis under analysis (i.e. the event is present or not). The function of the observed samples is often referred to as the *test statistic* for the problem at hand, and it can be obtained applying different optimization criteria. For instance, the well-known Neyman–Pearson (NP) criterion, which aims at maximizing the probability of detection subject to some probability of false alarm; the Generalized Likelihood Ratio Test (GLRT), which replaces unknown parameters by their maximum likelihood estimates (MLE); or the Bayesian criterion, which aims at minimizing a weighted function of different error probabilities, known as the Bayesian risk [1].

When it comes to assess the detection performance, the first step is to determine the density of the test statistic, or more specifically, its cumulative density function (cdf) also referred here as the *distribution*. This allows the designer to assess the receiver operating characteristics (ROC) based on the probability of (missed) detection and probability of false alarm, thus having a full picture of the overall detection performance [2].

In many real life applications dealing with Gaussian distributed samples, the resulting test statistic is based on homogeneous quadratic forms. That is to say, quadratic forms that are composed of linear combinations of quadratic terms or mixtures of both quadratic and crossed terms. Unfortunately, a closed-form expression cannot be obtained for the general class of homogeneous quadratic forms, since the presence of linearly combined correlated terms often makes the problem mathematically intractable. This is the case of tests statistics based on the weighted sum of chi-squared random variables, which have received significant attention in the past decades in the context of spacecraft engineering [3], transient signal detection [4], multiuser interference in broadcast channels, or cooperative spectrum sensing in wireless communications [5]. Because of the difficulty in characterizing linear combinations of quadratic forms, the resulting distribution is numerically computed through approximate methods such as the saddle-point approximation [6] or by matching a few of the first cumulants to some other known closed-form distributions [7].

☆ This work was partly supported by the Spanish Government under grant TEC2014-53656-R.

* Corresponding author.
E-mail addresses: daniel.egea@uab.es (D. Egea-Roca), gonzalo.seco@uab.es (G. Seco-Granados), jose.salcedo@uab.es (J.A. López-Salcedo).

https://doi.org/10.1016/j.dsp.2018.02.012
1051-2004/

The problem is further aggravated when dealing with *inhomogeneous* quadratic tests, where apart from a combination of quadratic forms, linear terms are also present thus making even more challenging to characterize the overall statistical distribution. Inhomogeneous quadratic forms appear in diverse applications such as neuron receptive fields modeling [8], financial problems dealing with portfolio losses of CDO pricing [9], or Signal Quality Monitoring (SQM) in Global Navigation Satellite Systems (GNSS) [10], just to mention a few. The use of inhomogeneous quadratic forms has typically remained in the realm of estimation and optimization theory, where the focus is placed on estimating unknown parameters or solving some optimization cost function [11]. To the best of the authors' knowledge, little attention has been paid to inhomogeneous quadratic tests in signal detection problems, where finding the statistical characterization of these tests is actually the cornerstone for solving the problem.

Motivated by this observation, the goal of this work is the derivation of closed-form approximations for the distribution of inhomogeneous quadratic forms, in order to facilitate the computation of the error probabilities in signal detection problems with time-varying working conditions. This is a fundamental problem in many real life applications, thus making the present contribution interdisciplinary and relevant to a wide audience. To illustrate the contribution, and without loss of generality, the example of transient change detection (TCD) is considered in the context of GNSS SQM. This is an application where the propagation conditions may vary quite rapidly, and the user terminal needs to promptly react to detect the presence of deleterious effect such as multipath [12], non-line-of-sight (NLOS) or signal attenuation [13], as well as potential threats such as spoofing [14] and interference attacks [15]. For illustration purposes, we will consider some generic SQM metric exhibiting a simultaneous change in mean and variance when some threat or signal distortion appears. The detection of this change results in an inhomogeneous quadratic test that fits very well with the ultimate motivation of this paper, which is nothing but to show the application of the proposed closed-form bounds in a practical case of interest.

The core of this work is based on exploiting the Edgeworth series expansion, which provides an analytical expression for the density of a random variable based on its constituent moments [16, p. 169]. In contrast to other methods, such as the saddle-point approximation, the advantage of the Edgeworth expansion is that it does not require the cumulant generating function to be known in closed-form [17]. Furthermore, it provides a closed-form expression to work with, which greatly simplifies its application in practical problems [18]. However, tailoring the Edgeworth expansion for the problem at hand is not straightforward, since it requires a specific truncation and a rather cumbersome computation of the required Hermite coefficients. In this context, the contributions of this work are twofold. Firstly, to overcome these concerns, the Edgeworth expansion for the problem at hand is computed. Moreover, it is shown that this expansion is accurate enough to approximate the miss detection probability of inhomogeneous quadratic tests in TCD problems. Secondly, it is also shown that the Edgeworth expansion is not so accurate when approximating the probability of false alarm. In that case, we will propose an alternative approximation based on results from Extreme Value Theory (EVT), which again make use of the statistics of inhomogeneous quadratic forms. The overall contribution of this work is to show that the proposed Edgeworth and EVT approximations provide a dual approach to assess the performance of signal change detectors dealing with inhomogeneous quadratic forms, while providing guidelines for their use and tuning in practical applications.

The paper is organized as follows. Some preliminaries are discussed in Section 2, where the signal model for inhomogeneous quadratic tests is provided as well as some stepping-stone results. Next, inhomogeneous quadratic test in TCD is introduced in Section 3. Closed-form approximations for the probability of miss and probability of false alarm are provided in Section 4 and Section 5, making use of Edgeworth series and EVT, respectively. The application example on GNSS SQM is discussed in Section 6, and finally, conclusions are drawn in Section 7.

2. Preliminaries

Let $\{Y_n\}_{n\geq 1}$ be a sequence of iid signal samples whose inner structure is given by the inhomogeneous quadratic form,

$$Y_n \doteq aX_n^2 + bX_n + c \tag{1}$$

for some constants $\{a, b, c\}$ and X_n some random variable. Because of the presence of a quadratic and a linear term, the density of Y_n is not straightforward. This problem is further aggravated when considering the sum of $\{Y_n\}_{n=1}^m$ signal samples,

$$Z \doteq \sum_{n=1}^{m} Y_n \tag{2}$$

whose density f_Z involves m times the convolution of the density of Y_n. This poses insurmountable obstacles for the derivation of a closed-form expression for f_Z, and the corresponding distribution, F_Z. In order to circumvent this limitation, the corresponding Edgeworth and EVT approximations will be derived, which provide a tight match to the original density while still providing a mathematically tractable and closed-form formulation. We will briefly recall here the Central Limit Theorem, which becomes a simple reference benchmark for the approximations to be proposed later on, as well as some indications on the statistical moments of Z to be used as well.

2.1. Central limit theorem (CLT) for the density of Z

Theorem 1 *(CLT). Let Z be the sum of m independent random variables $Y_1, Y_2, \ldots, Y_m$, with mean $\mu_Z = \mu_1 + \mu_2 + \ldots + \mu_m$ and variance $\sigma_Z^2 = \sigma_1^2 + \sigma_2^2 + \ldots + \sigma_m^2$. Then,*

$$f_Z(z) \xrightarrow[m\to\infty]{} \phi(\tilde{z}) \doteq \frac{1}{\sqrt{2\pi}} e^{-\tilde{z}^2/2} \tag{3}$$

$$F_Z(z) \xrightarrow[m\to\infty]{} \Phi(\tilde{z}) \doteq \frac{1}{\sqrt{2\pi}} \int_{-\infty}^{\tilde{z}} e^{-\lambda^2/2} d\lambda \tag{4}$$

with $\tilde{z} \doteq (z - \mu_Z)/\sigma_Z$, $\phi(\tilde{z})$ the standard Gaussian density and $\Phi(\tilde{z})$ the standard Gaussian distribution [19].

2.2. Moments of Z

Lemma 1. *Let $Z \doteq \sum_{n=1}^m Y_n$ with $\{Y_n\}_{n=1}^m$ independent random samples. The k-th order moment of Z can be computed using the multinomial theorem [20] as follows,*

$$\xi_Z^k \doteq \mathrm{E}\left[Z^k\right] = \sum_{l_1+l_2+\ldots+l_m=k} \frac{k!}{l_1!l_2!\cdots l_m!} \xi_{Y_1}^{l_1} \xi_{Y_2}^{l_2} \cdots \xi_{Y_m}^{l_m} \tag{5}$$

for all sequences $\{l_n\}_{n=1}^m \in \mathbb{Z}^*$ such that their sum is equal to k, and where ξ_Y^l stands for the l-th order moment of the inhomogeneous quadratic form in (1).

The computation of moments up to order four will be used later on, so it is convenient to provide the result here. After some cumbersome manipulations, the result is

$$\xi_Z = m\xi_Y \tag{6}$$

$$\xi_Z^2 = m\left[\xi_Y^2 + (m-1)(\xi_Y)^2\right] \tag{7}$$

$$\xi_Z^3 = m\left[\xi_Y^3 + (m-1)\left[3\xi_Y^2\xi_Y + (m-2)(\xi_Y)^3\right]\right] \tag{8}$$

$$\xi_Z^4 = m\Big[\xi_Y^4 + (m-1)\big[4\xi_Y^3\xi_Y + 3(\xi_Y^2)^2 + (m-2)\big[6\xi_Y^2(\xi_Y)^2 + (m-3)(\xi_Y)^4\big]\big]\Big]. \tag{9}$$

2.3. Moments of Y_n

Lemma 2. *Let $Y_n \doteq aX_n^2 + bX_n + c$ for some constants $\{a, b, c\}$ and some random variable X_n. Then the moments of Y_n are given by*

$$\xi_Y^k \doteq \mathrm{E}[Y_n^k] = \sum_{i=0}^{k} A(i), \tag{10}$$

with

$$A(i) \doteq \sum_{j=0}^{i} \binom{k}{i}\binom{i}{j} a^{k-i} b^{i-j} c^j \xi_{X,2k-i-j}, \tag{11}$$

where $\xi_X^k \doteq \mathrm{E}[X_n^k]$ is the k-th order moment of X_n and $\binom{l}{i} \doteq k!/(i!(k-i)!)$ is the binomial coefficient.

Proof. Let us rewrite Y_n as $Y_n = u + v$, with $u \doteq aX_n^2$ and $v \doteq bX_n + c$. Applying the binomial expansion gives

$$Y_n^k = \sum_{i=0}^{k} \binom{k}{i} u^{k-i} v^i = \sum_{i=0}^{k} \binom{k}{i} a^{k-i} X_n^{2(k-i)} (bX_n + c)^i. \tag{12}$$

Proceeding in the same way for the right-hand side of (12),

$$\begin{aligned} Y_n^k &= \sum_{i=0}^{k} \binom{k}{i} a^{k-i} X_n^{2(k-i)} \left(\sum_{j=0}^{i} \binom{i}{j} (bX_n)^{i-j} c^j \right) \\ &= \sum_{i=0}^{k} \sum_{j=0}^{i} \binom{k}{i}\binom{i}{j} a^{k-i} b^{i-j} c^j X_n^{2k-i-j} \end{aligned} \tag{13}$$

which leads to (10) once the expectation is applied. □

3. Inhomogeneous quadratic tests in transient change detection problems

This section tackle with signal decision metrics relying on inhomogeneous quadratic tests, as it is the case in many signal processing applications dealing with finance, biomedical engineering or positioning systems. Without loss of generality, the problem of TCD is considered, where the goal is to promptly detect the presence of an abnormal event in the observed signal. This problem has been widely studied in the existing literature [21], but no results are available for the case of inhomogeneous quadratic decision rules. In that sense, the present work is filling this gap by providing simple closed-form approximations to assess the performance of such decision rules. To do so, we will first introduce in Section 3.1 the Gaussian mean-and-variance change model (MVCM) widely adopted in many applications. Then Section 3.2 will show how inhomogeneous quadratic forms arise in the problem under study. Finally, Section 3.3 will introduce the detection performance metrics to be evaluated and the distributions whose closed-form expression is sought. The application to TCD presented in this section is for the sake of exemplification. The theoretical findings in this paper are valid for any other application dealing with inhomogeneous quadratic forms of Gaussian random variables.

3.1. Signal model

Let $\{X_n\}_{n\geq 1}$ be a sequence of random signal samples that are observed sequentially. Let us also consider a family $\{\mathbb{P}_\nu | \nu \in [1, 2, \ldots, \infty]\}$ of probability measures, such that under $\mathbb{P}_\nu$, the samples $X_1, \ldots, X_{\nu-1}$ and $X_{\nu+m}, \ldots, X_\infty$ are iid with a fixed marginal density $f_{X,0}$, with ν the deterministic but unknown change time when a change in density appears. On the other hand, $X_\nu, \ldots, X_{\nu+m-1}$ are iid with another marginal density $f_{X,1} \neq f_{X,0}$. In our case, we focus on the simultaneous change of mean and variance of a Gaussian density,

$$X_n \sim \begin{cases} \mathcal{H}_0: & \mathcal{N}(\mu_0, \sigma_0^2) \quad \text{if } 1 \leq n < \nu \text{ or } n \geq \nu + m \\ \mathcal{H}_1: & \mathcal{N}(\mu_1, \sigma_1^2) \quad \text{if } \nu \leq n < \nu + m \end{cases}, \tag{14}$$

where $\{\mu_0, \sigma_0^2\}$ are the mean and variance of X_n under nominal conditions (i.e. hypothesis $\mathcal{H}_0$) and $\{\mu_1, \sigma_1^2\}$ the mean and variance after the change (i.e. hypothesis $\mathcal{H}_1$). The model in (14) implicitly assumes that the random samples are sufficiently well represented by a stationary random process under $\mathcal{H}_0$ and $\mathcal{H}_1$. In practice, a pragmatic (and suboptimal) approach to detect non-stationary random samples under $\mathcal{H}_1$ is to set the corresponding mean and variances with the worst-case values to be detected. Typically, the smallest mean and variance that may be experienced under $\mathcal{H}_1$.

3.2. Test statistic

The detection of a transient change in the observed signal is completely defined by the *stopping time* T at which the change is declared, which can be computed following different rules and criteria [22, Ch. 6]. Herein the focus is on the finite moving average (FMA) stopping time introduced in [21] for the specific case of Gaussian mean-changes, and recently extended to the case of Gaussian mean- and variance-changes in [23]. The FMA test statistic results in the following stopping time

$$T_{\mathrm{F}} \doteq \inf\{n \geq m : S_n \geq h\}, \tag{15}$$

with h the detection threshold and

$$S_n \doteq \sum_{k=n-m+1}^{n} \mathrm{LLR}_k, \tag{16}$$

where $\mathrm{LLR}_k \doteq \ln\left(f_{X,1}(X_k)/f_{X,0}(X_k)\right)$ is the log-likelihood ratio (LLR) of the sample X_k. Interestingly, the LLR turns out to be an inhomogeneous quadratic form when evaluated for the signal model in (14). That is,

$$\mathrm{LLR}_k = aX_k^2 + bX_k + c \tag{17}$$

where the constants $\{a, b, c\}$ are given by:

$$a = \frac{\sigma_1^2 - \sigma_0^2}{2\sigma_0^2\sigma_1^2}, \tag{18}$$

$$b = \frac{\sigma_0^2\mu_1 - \sigma_1^2\mu_0}{\sigma_0^2\sigma_1^2}, \tag{19}$$

$$c = \ln\left(\frac{\sigma_0^2}{\sigma_1^2}\right) + \frac{\sigma_1^2\mu_0^2 - \sigma_0^2\mu_1^2}{2\sigma_0^2\sigma_1^2}. \tag{20}$$

The detection metric in (16) is actually the accumulation of m inhomogeneous quadratic forms, and therefore it can be modeled by the random variable Z in (2). While the exact density of (16) is unknown, the statistical moments can be derived using the results from Lemma 1 and 2.

3.3. Detection performance

The detection performance is measured in terms of the worst-case probability of missed detection and false alarm, which are defined respectively, as

$$\mathbb{P}_{\text{md}}(T_{\text{F}}) \doteq \sup_{\nu \geq 1} \mathbb{P}_{\nu}(T_{\text{F}} > \nu + m - 1 | T_{\text{F}} \geq \nu), \tag{21}$$

$$\mathbb{P}_{\text{fa}}(T_{\text{F}}) \doteq \sup_{l \geq 1} \mathbb{P}_{\infty}(l \leq T_{\text{F}} < l + m_{\alpha}), \tag{22}$$

where m is the length of the transient to be detected and m_{α} the time window where we want a given value of $\mathbb{P}_{\text{fa}}$ to be guaranteed. The exact computation of (21) and (22) leads to an intractable formulation. To circumvent this limitation, upper bounds are typically adopted instead such that [23],

$$\mathbb{P}_{\text{md}}(T_{\text{F}}) \leq \beta_m(h), \tag{23}$$

$$\mathbb{P}_{\text{fa}}(T_{\text{F}}) \leq \alpha_{m_{\alpha}}(h), \tag{24}$$

with

$$\beta_m(h) \doteq \mathbb{P}_1(S_n < h), \tag{25}$$

$$\alpha_{m_{\alpha}}(h) \doteq 1 - [\mathbb{P}_{\infty}(S_n < h)]^{m_{\alpha}}. \tag{26}$$

Due to the one-to-one relationship between (16) and (2), the upper bounds in (25)–(26) become

$$\beta_m(h) = F_{Z,1}(h) \tag{27}$$

$$\alpha_{m_{\alpha}}(h) = 1 - \left[F_{Z,0}(h)\right]^{m_{\alpha}} \tag{28}$$

with $F_{Z,0}$ and $F_{Z,1}$ the distribution of Z in the absence and in the presence of a transient signal change, respectively.

These distributions have no closed-form expression either, but tight approximations can be adopted instead. For instance, using the Edgeworth series expansion to be presented next in Section 4. This approach works well for $\beta_m(h)$ in (27), since it directly depends on the cumulative density function of Z, for which the Edgeworth expansion can readily be derived using the moments of Z in Section 2.2. However, some difficulties are found for $\alpha_{m_{\alpha}}(h)$ in (28) due to the presence of the m_{α}-th power on the cumulative density function of Z. In that case, the approximation errors incurred by the Edgeworth series tend to be amplified, thus potentially violating the upper bound inequality in (24). This issue will be addressed by adopting an alternative closed-form approximation using results from extreme value theory (EVT), as described next in Section 5.

4. Closed-form approximation for $\beta_m(h)$, the upper bound on $\mathbb{P}_{\text{md}}$

For a sufficiently large m, the density of Z in (2) can be assumed to be Gaussian in virtue of the CLT. This certainly relaxes the complexity of the problem at hand, and provides an acceptable match with the target density. However, the CLT approximation is often too loose for small m or when focusing on the tails of the resulting distribution, as it occurs when dealing with error probabilities (e.g. $\mathbb{P}_{\text{md}}$ and $\mathbb{P}_{\text{fa}}$). A tighter approximation can be obtained through the following theorem [24, p. 223]:

Theorem 2 *(Gram–Charlier type-A expansion). The error between the target density f_Z and the CLT approximation can be modeled by a series expansion as follows:*

$$\epsilon(\tilde{z}) \doteq f_Z(z) - \phi(\tilde{z}) = \phi(\tilde{z}) \sum_{p=3}^{\infty} \frac{C_p}{p!} H_p\left(\tilde{z}\right) \tag{29}$$

with $\tilde{z} \doteq (z - \mu_Z)/\sigma_Z$, $H_p(\tilde{z})$ the Hermite polynomial of degree p and C_p the projection of the target density onto $H_p(\tilde{z})$,

$$C_p \doteq \int_{-\infty}^{\infty} H_p\left(\tilde{z}\right) f_Z(\tilde{z}) d\tilde{z}. \tag{30}$$

Corollary 1 *(Gram–Charlier type-A expansion for f_Z). Using the result in (29), the density of Z can be represented through the following series expansion,*

$$f_Z(z) = \phi\left(\tilde{z}\right) \left[1 + \sum_{p=3}^{\infty} \frac{C_p}{p!} H_p\left(\tilde{z}\right)\right]. \tag{31}$$

Corollary 2 *(Gram–Charlier type-A expansion for F_Z). Integrating the result in (29), the distribution of Z can be represented through the following series expansion,*

$$F_Z(z) = \Phi\left(\tilde{z}\right) - \sigma_Z \phi(\tilde{z}) \sum_{p=3}^{\infty} \frac{C_p}{p!} H_{p-1}\left(\tilde{z}\right). \tag{32}$$

Proof. See Appendix A. □

While the results in (31)–(32) provide a closed-form approximation for $f_Z(z)$ and $F_Z(z)$, it is well-known that the Gram–Charlier approximation may suffer from some instabilities and convergence issues [25,16]. In particular, the terms of the infinite series in (29) do not monotonically decrease with increasing the order p, thus making the truncation of the asymptotic series a not trivial task. Notwithstanding, these issues can be circumvented by rearranging the error terms so as to provide a series expansion with guaranteed convergence [24]. This rearrangement of terms leads to the so-called Edgeworth series expansion, which consists on grouping the error terms with similar order. This is the case, for instance, of terms $p = 3$, $p = \{4, 6\}$ and $p = \{5, 7, 9\}$. Using this observation, we are now in position to provide a closed-form approximation for the upper bound on $\mathbb{P}_{\text{md}}$ in (27).

Proposition 1 *(Edgeworth approximation for $\mathbb{P}_{\text{md}}$). Using the result in (32), the upper bound on $\mathbb{P}_{\text{md}}$ in (27) can be approximated as follows*

$$\begin{aligned} \beta_m(h) &\approx \beta_{\text{EDG},m}(h) \\ &= \Phi(\tilde{h}_1) - \sigma_{Z,1} \phi(\tilde{h}_1) \sum_{p \in \mathcal{A}} C_{p,1} H_{p-1}(\tilde{h}_1) \end{aligned} \tag{33}$$

where $\mathcal{A} = \{3, 4, 6\}$ and $C_{p,1}$ are the Hermite coefficients computed using $f_{Z,1}(z)$ under $\mathcal{H}_1$, and given by

$$\begin{aligned} C_{3,1} &= \frac{\xi_{Z,1}^3 - 3\xi_{Z,1}\xi_{Z,1}^2 + 2(\xi_{Z,1})^3}{\sigma_{Z,1}^3}, \\ C_{4,1} &= \frac{\xi_{Z,1}^4 - 4\xi_{Z,1}\xi_{Z,1}^3 + 6(\xi_{Z,1})^2\xi_{Z,1}^2 - 3(\xi_{Z,1})^4}{\sigma_{Z,1}^4} - 3, \\ C_{6,1} &= 10C_{3,1}^2, \end{aligned} \tag{34}$$

where $\xi_{Z,1}^k$ is the k-th order moment of Z, which can be evaluated using the results in Section 2.2 under $\mathcal{H}_1$. Finally, $\sigma_{Z,1}$ is the standard deviation of Z that can be obtained as $\sigma_{Z,1} = \sqrt{\xi_{Z,1}^2 - (\xi_{Z,1})^2}$, and $\tilde{h}_1 \doteq (h - \xi_{Z,1})/\sigma_{Z,1}$.

5. Closed-form approximations for $\alpha_{m_\alpha}(h)$, the upper bound on $\mathbb{P}_{\text{fa}}$

5.1. Edgeworth series approximation

A closed-form approximation for the upper bound of $\mathbb{P}_{\text{fa}}$ in (28) can similarly be obtained substituting $F_{Z,0}$ by its Edgeworth series expansion, as already done in (33) for $\mathbb{P}_{\text{md}}$.

Proposition 2 *(Edgeworth approximation for $\mathbb{P}_{\text{fa}}$). Using the result in (32), the upper bound on $\mathbb{P}_{\text{fa}}$ in (28) can be approximated as follows*

$$\alpha_{m_\alpha}(h) \approx \alpha_{\text{EDG},m_\alpha}(h) = 1 - \left[\Phi(\tilde{h}_0) - \sigma_Z \phi(\tilde{h}_0) \sum_{p\in\mathcal{A}} C_{p,0} H_{p-1}(\tilde{h}_0)\right]^{m_\alpha} \tag{35}$$

where $\mathcal{A} = \{3, 4, 6\}$, $\tilde{h}_0 \doteq (h - \xi_{Z,0})/\sigma_{Z,0}$ and $C_{p,0}$ are the Hermite coefficients computed using $f_{Z,0}(z)$ under $\mathcal{H}_0$, and given by (34) replacing $\xi_{Z,1}$ by $\xi_{Z,0}$.

5.2. Extreme value theory (EVT) approximation

Although the Edgeworth series provides a better approximation for the tails of the density of Z than the CLT, there is still some mismatch between the tail of the approximation and the true density. This mismatch is negligible for the case of approximating $F_{Z,1}$ in (27), but it is not when approximating the m_α-th power of $F_{Z,0}$ in (28). The approximation inaccuracies become amplified and the upper bound inequality in (24) is not guaranteed to be preserved anymore.

In order to circumvent this issue an alternative approximation for $\mathbb{P}_{\text{fa}}$ will be formulated making use of results from extreme value theory (EVT). EVT has historically been linked to the statistical problem of flood frequency analysis, where predicting such extreme events is of paramount importance. However, EVT is also widely adopted today in applications dealing with finance, insurance or engineering [26]. In the problem at hand, the upper bound in (28) can be understood as the probability that none of the m_α trials of Z under $\mathcal{H}_0$ exceeds the threshold h. This is equivalent to state that the maximum of these m_α trials does not exceed it either. Following this rationale, the next theorem is used.

Theorem 3 *(EVT distribution). Let $U \doteq \max_{1\le i\le N}\{Z_i\}$ with $\{Z_i\}_{i=1}^N$ iid samples whose density f_Z exhibits exponentially decreasing tails. Let us also define*

$$\delta \doteq F_Z^{-1}\left(1 - \frac{1}{N}\right), \tag{36}$$

$$\gamma \doteq N f_Z(\delta). \tag{37}$$

Then, the distribution of U becomes

$$F_U(u) \overset{N\to\infty}{=} \exp\left(-e^{-\gamma(u-\delta)}\right). \tag{38}$$

Proof. See [26, p. 166]. □

Using the result above, an alternative approximation for the upper bound on $\mathbb{P}_{\text{fa}}$ follows.

Proposition 3 *(EVT approximation for $\mathbb{P}_{\text{fa}}$). Using the result in Theorem 1, the upper bound on $\mathbb{P}_{\text{fa}}$ in (28) can be approximated as follows*

$$\alpha_{m_\alpha}(h) \approx \alpha_{\text{EVT},m_\alpha}(h) = 1 - \exp\left(-e^{-\gamma_{m_\alpha}(h-\delta_{m_\alpha})}\right), \tag{39}$$

where

$$\delta_{m_\alpha} \doteq F_{Z,0}^{-1}\left(1 - \frac{1}{m_\alpha}\right), \tag{40}$$

$$\gamma_{m_\alpha} \doteq m_\alpha f_{Z,0}(\delta_{m_\alpha}). \tag{41}$$

Proof. The term $[F_{Z,0}(h)]^{m_\alpha}$ in (28) can be rewritten as

$$[F_{Z,0}(h)]^{m_\alpha} = \mathbb{P}_\infty\left(\bigcap_{i=1}^{m_\alpha} Z_i < h\right) = \mathbb{P}_\infty\left(M_{m_\alpha} < h\right), \tag{42}$$

with $M_{m_\alpha} \doteq \max_{1\le i\le m_\alpha}\{Z_i\}$. That is, $[F_{Z,0}(h)]^{m_\alpha}$ is obtained as the probability that m_α iid signal samples of Z are below the value h, which is equivalent to the probability that the maximum of all m_α samples is below h. Thereby, EVT can apply to obtain $[F_{Z,0}(h)]^{m_\alpha}$. Since Z is the sum of dependent non-central chi-squared and Gaussian random variables, the density of Z has an exponentially decreasing tail and Theorem 3 is applicable to (42). On the other hand, since the density and distribution of Z are unknown, the corresponding Edgeworth expansion is applied in order to use Theorem 3, and the proof of Corollary 3 thus follows. □

Before concluding this section it is worth noting that to obtain δ_{m_α} in (40) the inverse distribution $F_{Z,0}^{-1}$ needs to be evaluated. Even though there is no closed-form for this inverse, it can easily be found by numerically solving $F_{Z,0}(\delta) = 1 - (1/m_\alpha)$. This numerical evaluation is possible thanks to the proposed Edgeworth closed-form for $F_{Z,0}$ and the use of a simple iterative algorithm like the Newton–Raphson method, which can be easily implementable in a digital receiver. Once δ_{m_α} is calculated, the approximation in (39) can be applied to calculate $F_{Z,0}$ in a closed form. In case it was of interest to obtain the threshold guaranteeing a given level of false alarms $\tilde{\alpha}$, it can be fixed from (39) as

$$h(\tilde{\alpha}) = \delta_{m_\alpha} - \frac{\ln\left(-\ln\left(1-\tilde{\alpha}\right)\right)}{\gamma_{m_\alpha}}. \tag{43}$$

This procedure is very convenient to be used in practice within a digital receiver.

6. Application to signal quality monitoring in GNSS

Section 3 has introduced inhomogeneous quadratic tests in the context of TCD. Next, closed-form approximations for its statistical distribution have been proposed in Section 3 and 5, thus facilitating the computation of $\mathbb{P}_{\text{md}}$ and $\mathbb{P}_{\text{fa}}$ in practice. In the present section, these results will be applied to a particular case study such as the one of SQM in GNSS [27]. Without loss of generality, this example serves to illustrate the goodness of the proposed upper bounds on $\mathbb{P}_{\text{md}}$ in (33) and $\mathbb{P}_{\text{fa}}$ in (35) and (39). For simplicity, the former is denoted by β_{EDG} and the latter by α_{EDG} and α_{EVT}, respectively. It is worth clarifying that the used model can be regarded as a simplification of signal quality monitoring, as used in most of SQM contributions [14,28,29], and it is used here for the sake of exemplification. Nevertheless, if more sophisticated and accurate models are available they should be used instead.

6.1. Motivation

Integrity refers herein to the ability of a GNSS receiver to guarantee the quality and trust of the received signal in such a way that critical applications can be safely operated. While this concept is circumscribed here to GNSS, it can actually be extrapolated to many other disciplines where some element needs to be monitored for quality control purposes. In our case, signal processing

techniques must be implemented at the receiver side to analyze some key performance indicators of the received signal and to detect abnormal values. While this problem has been widely addressed within the civil aviation community [30], it has always remained at the realm of position, velocity and time (PVT) observables, where measurements from several sources need to be compared and cross-checked for consistency purposes. In the recent years, there has been an increasing interest in signal quality metrics. The reason is that they can act as early indicators on the presence of integrity threats, since they are metrics directly linked to the physical received signal and they are readily available before PVT observables are computed. This is the case of the signal-to-noise ratio (SNR), the symmetry of the correlation peak at the matched filter output, or the ratio between the maximum and minimum eigenvalues of the spatial correlation matrix in multi-antenna systems.

The problem to be addressed here fits perfectly within the scope of TCD, since the density of many signal quality measurements suddenly departs from its nominal value when some threat is present (e.g. a jamming signal, multipath reflections, etc.). Moreover, for integrity purposes, the delay to detect a threat is bounded by the so-called time-to-alert. In our model given by (14) the time-to-alert is modeled by m, so that a detection delayed more than m samples is considered missed, thus fitting with the framework of TCD. Furthermore, it is important to say that the parameters that govern the distribution under $\mathcal{H}_1$ may be unknown in practice or may not be stationary, as confirmed by several experimental data analyses [29,31]. Nevertheless, the pragmatic approach to cope with these situations is to set as change parameters under $\mathcal{H}_1$ in (14) those corresponding to the smallest change in mean and variance to be detected. This assumes that the distribution under $\mathcal{H}_1$ is sufficiently well represented by a stationary random process, as considered by many of the contributions on SQM in the existing literature [12,14,28,29]. We will follow this approach for the sake of simplicity, since we are merely interested in showing how to apply the proposed closed-form bounds for $\mathbb{P}_{\text{md}}$ and $\mathbb{P}_{\text{fa}}$ in a case of interest.

6.2. SQM with the Slope Asymmetry Metric (SAM)

Among the wide range of possible signal quality metrics, the focus here is on the so-called slope asymmetry metric (SAM) [32]. This metric is intended to detect some distortion of the correlation curve, which may be caused by propagation effects such as multipath, but also by the presence of counterfeit signals in spoofing attacks. The SAM metric is obtained at the output of the matched filter by comparing the left and right slopes of the cross-correlation between the GNSS received signal $r(k)$ and the local replica $c(k)$. To better illustrate the process, let us denote the cross-correlation output samples by $R(\hat{\tau}, \hat{f})$, which in general can be computed using a combination of coherent and noncoherent integrations as follows,

$$R(\hat{\tau}, \hat{f}; n) = \sum_{m=nN_{\text{I}}}^{(n+1)N_{\text{I}}-1} \left| \sum_{k=mL_{\text{C}}}^{(m+1)L_{\text{C}}-1} r(k)c(k-\hat{\tau})e^{-j2\pi \hat{f}k} \right|^2 \tag{44}$$

where $\{\hat{\tau}, \hat{f}\}$ are the tentative time-delay and Doppler frequency at the acquisition or tracking stage of the receiver, L_{C} is the coherent integration length and N_{I} the number of noncoherent integrations [33]. These correlation samples and the process to obtain the SAM through them is shown in Fig. 1. For a given side of the correlation peak, a set of discrete-time samples can be collected in the neighborhood of $\hat{\tau}$ and stack them into vector form, $\mathbf{r}(n) \doteq [R(\tau_1, \hat{f}; n), R(\tau_2, \hat{f}; n), \ldots, R(\tau_L, \hat{f}; n)]^T$, where $|\tau_i - \hat{\tau}| < T$

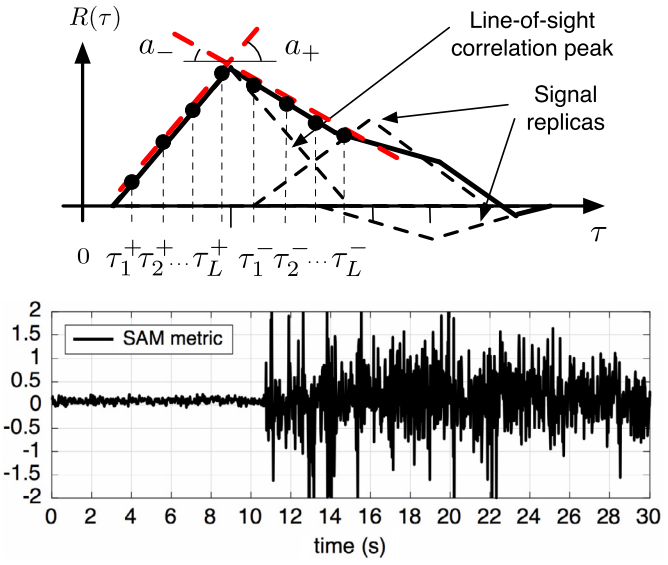

Fig. 1. (Up) Correlation peak of a GNSS received signal affected by some signal distortion. (Down) Example of SAM time series where distortion appears at $t = 11$ s.

for $i = 1, 2, \ldots, L$, and T usually given by the chip period of the GNSS signal. The fitting of these samples with a linear shape $R(\tau, f; n) \approx a(n)\tau + b(n)$, for some constants $\{a(n), b(n)\}$, can be formulated as a least squares estimation problem where the slope is obtained as,

$$\hat{a}(n) = \left[(\mathbf{M}^H\mathbf{M})^{-1}\mathbf{M}^H\mathbf{r}(n) \right]_{1,1} \tag{45}$$

where $[\cdot]_{i,j}$ denotes the (i, j) element, and $\mathbf{M}$ is given by

$$\mathbf{M} \doteq \begin{bmatrix} \tau_1 & \tau_2 & \ldots & \tau_L \\ 1 & 1 & & 1 \end{bmatrix}^T. \tag{46}$$

The solution in (45) must be evaluated twice, using correlation samples from each of the sides of the correlation peak. That is, with either $\{\tau_1^+, \tau_2^+, \ldots, \tau_L^+\}$ or $\{\tau_1^-, \tau_2^-, \ldots, \tau_L^-\}$ as illustrated in Fig. 1, in order to obtain the estimates of the left and right slopes of the correlation peak, respectively. These slopes are denoted by the pair $\{\hat{a}_+(n), \hat{a}_-(n)\}$ in Fig. 1 and they lead to the so-called SAM metric, which is obtained as

$$\text{SAM}(n) \doteq \hat{a}_+(n) + \hat{a}_-(n). \tag{47}$$

In nominal conditions when only the line-of-sight signal is received, the correlation peak should exhibit a nearly symmetric shape, thus causing the SAM to become a zero mean random process. However, when a threat introducing some signal distortion is present, the right slope of the correlation peak tends to flatten thus causing the SAM to depart from zero mean. A detailed analysis of the SAM metric was conducted in [34] using experimental data, where it was shown that (47) could fairly be modeled by the same Gaussian MVCM as in (14). Similar models are adopted in [12] and [28] for similar metrics As such, detecting a sudden change in the SAM metric using the FMA stopping rule in (15) leads to the same inhomogeneous quadratic form as in (17). Therefore, the detection performance can be assessed using the upper bounds in Section 3.3, whose closed-form expressions are proposed in Section 6.3 for $\mathbb{P}_{\text{md}}$ and in Section 6.4 for $\mathbb{P}_{\text{fa}}$. It is important to emphasize here that detecting changes in the SAM metric is just one of the possible applications where the proposed closed-form approximations for $\mathbb{P}_{\text{md}}$ and $\mathbb{P}_{\text{fa}}$ can be used. In practice, many other problems can be formulated in terms of the inhomogeneous

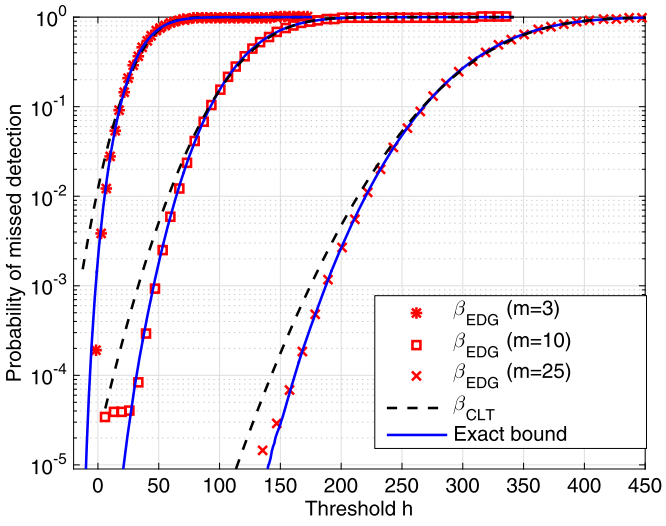

Fig. 2. Comparison between the exact bound for the probability of missed detection $\beta_m(h)$ with the corresponding Edgeworth and the CLT approximation for $m = \{3, 10, 25\}$.

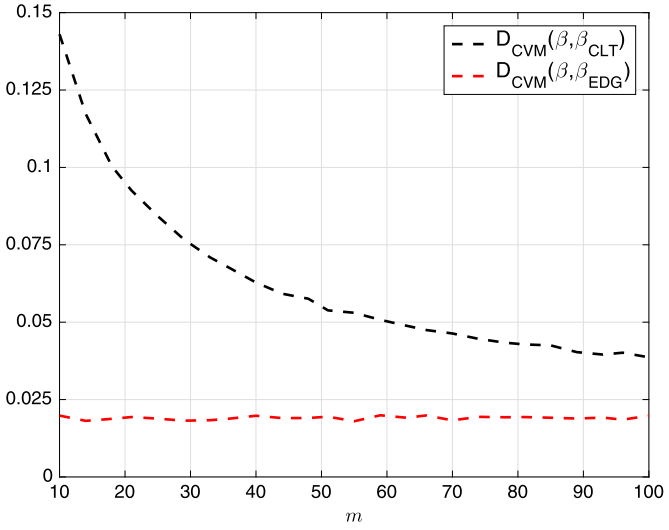

Fig. 3. Cramér–von Mises distance between the exact bound for the probability of missed detection β and the Egeworth and CLT approximations $\{\beta_{CLT}, \beta_{EDG}\}$ for the range of interest $0 \leq \beta \leq 0.1$.

quadratic test in (17), and therefore our contribution would be applicable too.

For the results to be shown next, we consider a GNSS receiver operating in a representative urban scenario where abnormal propagation conditions appear. According to the measurement campaign conducted in [10], the following values have been used for the Gaussian MVCM in (14) when applied to the SAM metric: $\mu_0 = 10^{-1}$, $\mu_1 = 2 \cdot 10^{-1}$, $\sigma_0^2 \in [10^{-4}, 10^{-2}]$ and $\sigma_1^2 \in [10^{-3}, 10^{-2}]$, where SAM samples are provided at sampling time $T_s = 1$ second. Without loss of generality, values within these ranges will be used when assessing the goodness of the Edgeworth approximation for the upper bound on $\mathbb{P}_{md}$ in Section 6.3. Next, the upper bound on $\mathbb{P}_{fa}$ in Section 6.4 will follow, where both the Edgeworth and EVT approximations will be compared. Apart from the computation of the corresponding probabilities, the distance between the exact bound and each of the proposed approximations will be also evaluated. This will be done using the Cramér–von Mises distance [35],

$$D^2_{CVM}(F, \widehat{F}) \doteq \int_{-\infty}^{\infty} \left(F(h) - \widehat{F}(h)\right)^2 dF(h) \tag{48}$$

where $F(h)$ stands for the exact bound distribution, $\alpha_{m_\alpha}(h)$ or $\beta_m(h)$, and $\widehat{F}(h)$ stands for the proposed approximations. The normalized distance is here computed following [36].

6.3. Goodness of the upper bound on $\mathbb{P}_{md}$

Fig. 2 shows the comparison between the exact bound $\beta_m(h)$ in (27) and both the CLT and Edgeworth approximations for different values of the transient duration, $m = \{3, 10, 25\}$ samples. The signal parameters for the MVCM are $\mu_0 = 10^{-1}$, $\sigma_0^2 = 4 \cdot 10^{-4}$, $\mu_1 = 2 \cdot 10^{-1}$, $\sigma_1^2 = 1.6 \cdot 10^{-3}$. The results in Fig. 2 show a tight match between the proposed Edgeworth approximation and the exact bound, even for low values of m, in contrast to what happens with the CLT approximation. The tight match is particularly true for moderate values of probability of miss down to 10^{-4}, which comprise the region where practical algorithms typically operate. Some inaccuracies are observed for the Edgeworth approximation, but they are restricted to low values of m and $\beta_m(h) < 10^{-4}$.

For the same signal parameters, the Cramér–von Mises distance between the exact bound and the proposed approximations is depicted in Fig. 3 as a function of the transient length. The results were obtained for $0 \leq \beta \leq 0.1$, which is the range of missed detections that are typically considered in practical applications. As can be observed in Fig. 3, the Edgeworth approximation is consistently providing a better match to the exact distribution, when compared to the CLT. It is true though that the accuracy of the CLT approximation improves with the transient length, as more terms are accumulated in (16). However, the transient would need to be on the order of a few hundred samples length for the CLT to provide similar results to the Edgeworth approximation in terms of probability of miss detection.

6.4. Goodness of the upper bound on $\mathbb{P}_{fa}$

Two experiments are considered: the first one for different values of the transient length $m = \{3, 10, 25, 50\}$ and $m_\alpha = 10m$ as the time window for guaranteed $\mathbb{P}_{fa}$; the second one for a fixed transient length $m = 6$ and two possible time windows for guaranteed $\mathbb{P}_{fa}$, namely $m_\alpha = \{60, 900\}$. The latter correspond to 1 and 15 minutes time windows commonly adopted in some integrity applications.

The results for the first experiment are shown in Fig. 4, illustrating the match between the Edgeworth approximation and the exact bound $\alpha_{m_\alpha}(h)$ is not that tight as the one previously discussed in Section 6.3 for $\beta_m(h)$. Indeed, there are values of the threshold h where the Edgeworth approximation is actually below the exact bound, thus violating the upper-bound inequality in (24). This is indeed the main reason for the proposed EVT approximation, which is shown in Fig. 4 to always remain above the exact bound, thus fulfilling the upper-bound inequality.

Examining the behavior of both the Edgeworth and EVT approximations as a function of m, it is seen that the greater the value of m, the slightly closer both approximations are to the exact bound. For the Edgeworth approximation, this behavior is due to the fact that the distribution is improved as m increases. However, since the m_α-th power of this approximation has to be computed in (28), the error terms are still amplified and they cause the overall approximation to violate the inequality in (24). This effect is not observed when using the EVT approximation, which is directly approximating the m_α-th power of the distribution and turns out to preserve the upper-bound inequality in (28).

Fig. 5 shows the Cramér–von Mises distance between the exact bound α_{m_α} and the Edgeworth and EVT approximations

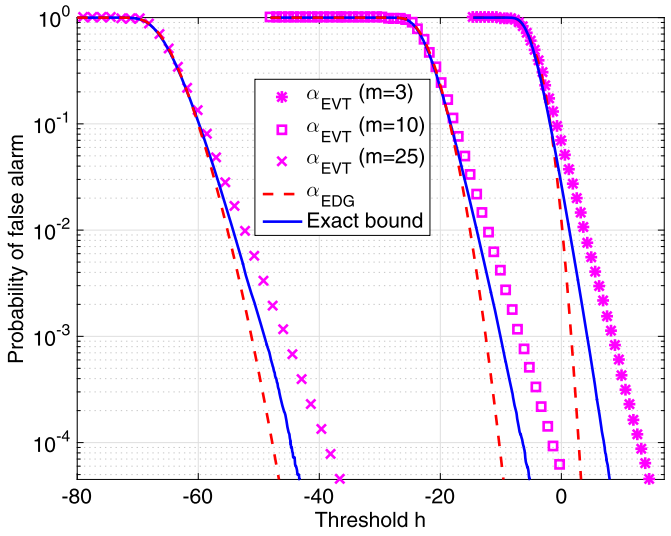

Fig. 4. Comparison between the exact bound for the probability of false alarm $\alpha_{m_\alpha}(h)$ with the corresponding Edgeworth and the EVT approximation for $m = \{3, 10, 25\}$ and $m_\alpha = 10 \cdot m$.

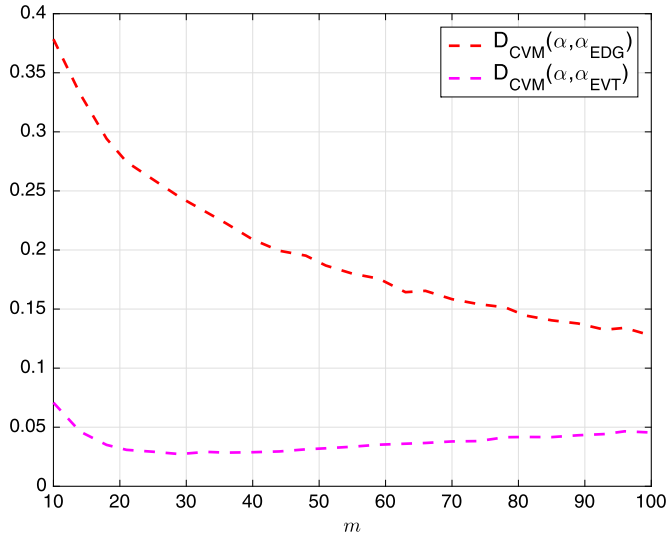

Fig. 5. Cramér–von Mises distance between the exact bound for the probability of false alarm α and the Edgeworth and EVT approximations $\{\alpha_{EDG}, \alpha_{EVT}\}$ for the range of interest $0 \leq \alpha \leq 0.1$.

$\{\alpha_{EDG}, \alpha_{EVT}\}$, as a function of m. Since low probabilities of false alarm are of interest, the results in Fig. 5 have been computed within the range of values $0 \leq \alpha \leq 0.1$ (i.e. focusing on the tails of the distributions under analysis). As shown, the EVT approximation is always providing the closest match to the exact bound, with a quite constant behavior as a function of m. The results for the Edgeworth approximation tend to improve for large values of m, due to the larger accumulation of terms in (16). Nevertheless, the overall distance with respect to the exact bound is still larger than the one achieved by EVT.

The results for the second experiment with fixed m_α corresponding to a 1 and 15 minutes time window are shown in Fig. 6. The upper plot shows that for $m_\alpha = 60$ the Edgeworth approximation is closer to the exact bound than the EVT one, even in the tail. Nonetheless, the Edgeworth approximation is below the exact bound for $h > 2$. This is an undesirable behavior that prevents us from using this approximation for upper-bounding $\mathbb{P}_{fa}$. On the other hand, the lower plot shows how for a larger value, $m_\alpha = 900$, the Edgeworth approximation provides worse results due to the

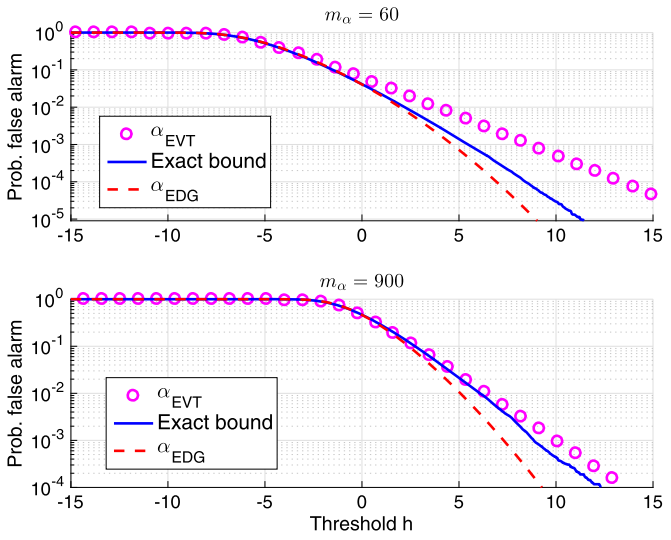

Fig. 6. Comparison between the exact bound for the probability of false alarm with the corresponding Edgeworth and EVT approximation for $m_\alpha = \{60, 900\}$ and fixed $m = 6$.

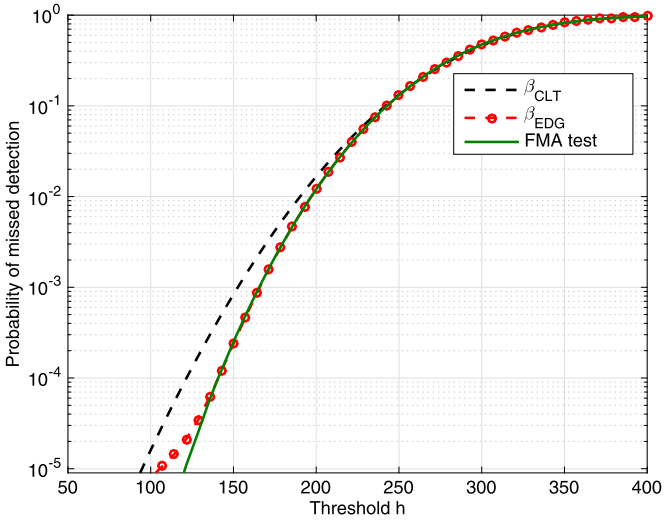

Fig. 7. Comparison between the true $\mathbb{P}_{md}(T_F)$ and the proposed approximations for the FMA stopping time test.

impact of the m_α-th power, whereas the EVT approximation actually improves when increasing m_α for a fixed m.

6.5. Performance assessment of the FMA stopping test

Once the goodness of the proposed approximations for $\beta_m(h)$ and $\alpha_{m_\alpha}(h)$ has been presented, the next step is to assess the performance of the FMA test. To do so, the true $\mathbb{P}_{md}(T_F)$ and $\mathbb{P}_{fa}(T_F)$ for the FMA test in (15) have been numerically evaluated and compared with the proposed approximations. The results can be observed first in Fig. 7 for $\mathbb{P}_{md}$ as a function of the detection threshold h. It is shown that the CLT approximation clearly departs from the true $\mathbb{P}_{md}(T_F)$ for probabilities smaller than 10^{-2}. In contrast, the Edgeworth approximation provides a really tight match with the true $\mathbb{P}_{md}(T_F)$ for values down to 10^{-4}, thus providing a two-orders-of-magnitude improvement with respect to the CLT. Results for $\mathbb{P}_{fa}$ are shown in Fig. 8, in which is shown that the Edgeworth approximation fulfills the upper-bound down to a probability of 10^{-2}, only. In contrast, the EVT approximation permanently upper-bounds $\mathbb{P}_{fa}(T_F)$ in the whole range of probabil-

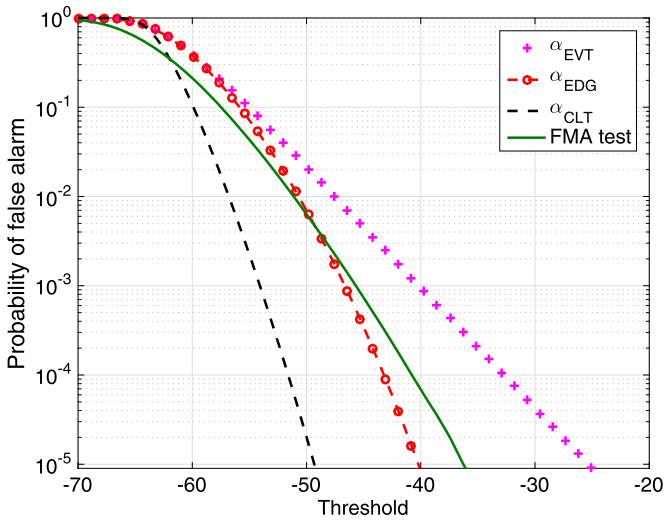

Fig. 8. Comparison between the true $\mathbb{P}_{fa}(T_F)$ and the proposed approximations for the FMA stopping time test.

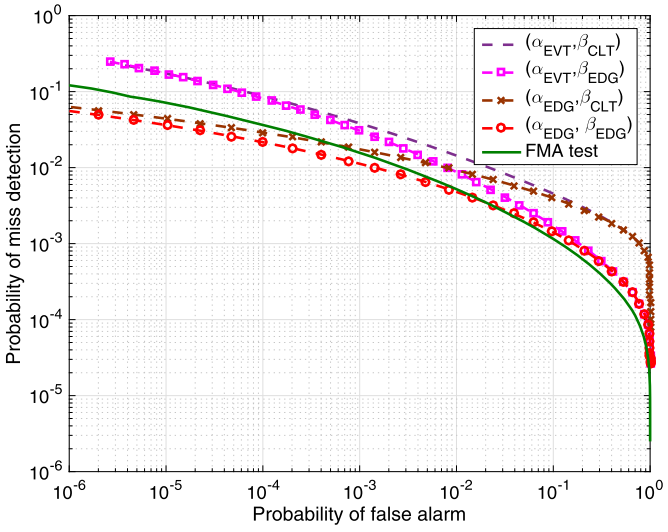

Fig. 9. Comparison between the numerical and the approximated ROC using combinations of either α_{EVT} in (39) or α_{EDG} in (35), with β_{CLT} in (4) or β_{EDG} in (33).

ities. The results have been obtained using the same parameters as for Fig. 2 but with $m = 6$, $m_\alpha = 60$, and $\mu_1 = 0.3$.

Finally, the results from $\mathbb{P}_{md}$ and $\mathbb{P}_{fa}$ are combined to build the receiver operating characteristics (ROC) shown in Fig. 9. Please note that this definition of ROC is different from the standard one, since probability of missed detection is considered here instead of probability of detection. The same parameters as in Fig. 6 have been used with $m = 6$ and $m_\alpha = 300$, and the true (i.e. numerical) results are compared with the different approximations presented so far in this work. That is, the Edgeworth and EVT approximations for the bound on $\mathbb{P}_{fa}(T_F)$ (i.e. α_{EVT} and α_{EDG}), and the CLT and Edgeworth approximations for the bound on $\mathbb{P}_{md}(T_F)$ (i.e. β_{EDG} and β_{CLT}). Results are shown in Fig. 9 for all possible pairs of approximations, namely $\{\alpha_{EVT}, \beta_{CLT}\}$, $\{\alpha_{EVT}, \beta_{EDG}\}$, $\{\alpha_{EDG}, \beta_{CLT}\}$ and $\{\alpha_{EDG}, \beta_{EDG}\}$.

The best upper bound approximation to the FMA test performance is sought, and for the case under study, the best upper bound is provided by the pair $\{\alpha_{EVT}, \beta_{EDG}\}$ as seen in Fig. 9. This is the pair providing the uniformly closest upper bound to the true FMA performance. Some other pairs provide a closer upper bound, but just for a finite range of missed detection or false alarm probabilities. This is therefore a clear example showing the interest in the use of the proposed Edgeworth and EVT approximations for inhomogeneous detection problems, which span outside the domain of the specific application on GNSS SQM considered herein.

7. Conclusions

This work has focused on inhomogeneous quadratic tests, which comprise the sum of dependent chi-square and Gaussian random variables and arise in many diverse fields such as biomedicine, finance or engineering. The main drawback of these tests is that their statistical characterization has no closed-form expression, and this poses serious troubles for their application in detection problems where error probabilities need to be computed. In order to circumvent this limitation, closed-form approximations for the probability of miss detection and probability of false alarm have been proposed making use of results from EVT and Edgeworth series expansions. Light has been shed on their practical computation and their performance have been assessed in a practical case study dealing with transient change detection in GNSS signal quality monitoring. Simulation results have been obtained using realistic parameters in order to assess the goodness of the proposed approximations, and the superior performance with respect to the widely adopted approximation relying on the CLT. While the application was kept in the context of GNSS, the results are general and guidelines are provided for their application to any other field where inhomogeneous quadratic tests need to be evaluated.

Appendix A. Proof of Corollary 2

Lemma 3. *Let $H_p(\tilde{z})$ be the Hermite polynomial of degree p, then*

$$\left(\frac{d}{d\tilde{z}}\right)^p \phi(\tilde{z}) = (-1)^p H_p(\tilde{z})\phi(\tilde{z}). \tag{49}$$

Proof. First, note that $\phi(\tilde{z}) \doteq e^{-\tilde{z}^2/2}/\sqrt{2\pi}$, and then

$$\begin{aligned} e^{-\tilde{z}^2/2} &= \sqrt{2\pi}\phi(\tilde{z}), \\ e^{\tilde{z}^2/2} &= \left(\sqrt{2\pi}\phi(\tilde{z})\right)^{-1}. \end{aligned} \tag{50}$$

On the other hand, the Hermite polynomials are defined as

$$H_p(\tilde{z}) \doteq (-1)^p e^{\tilde{z}^2/2}\left(\frac{d}{d\tilde{z}}\right)^p e^{-\tilde{z}^2/2}. \tag{51}$$

Hence, substituting (50) into (51) yields

$$H_p(\tilde{z}) = (-1)^p(\phi(\tilde{z}))^{-1}\left(\frac{d}{d\tilde{z}}\right)^p \phi(\tilde{z}), \tag{52}$$

which leads to (49). □

The proof of Corollary 1 follows straight away from the Taylor series expansion of $f_Z(\tilde{z})$ and the orthogonal properties of the Hermite polynomials [24]. However, some further manipulations are required to proof Corollary 2. Starting from the distribution definition, it follows that

$$\begin{aligned} F_Z(z) &\doteq \int_{-\infty}^{z} f_Z(u)du \\ &\approx \Phi(\tilde{z}) + \sum_{p=3}^{\infty}\frac{C_p}{p!}\int_{-\infty}^{z}\phi(\tilde{u})H_p(\tilde{u})du, \end{aligned} \tag{53}$$

where $\tilde{u} \doteq (u - \mu_Z)/\sigma_Z$ and the first term follows by the definition of the standard Gaussian distribution. The integral is solved by integrating (49),

$$\int_{-\infty}^{z} \phi(\tilde{u}) H_p(\tilde{u}) du = \sigma_z \int_{-\infty}^{z} (-1)^p \left(\frac{d}{d\tilde{u}}\right)^p \phi(\tilde{u}) d\tilde{u} \qquad (54)$$
$$I = \sigma_z (-1)^p \left[\left(\frac{d}{d\tilde{u}}\right)^{p-1} \phi(\tilde{u})\right]_{-\infty}^{z},$$

where the first equality follows by applying a change of variable. On account of (49) it follows that

$$\int_{-\infty}^{z} \phi(\tilde{u}) H_p(\tilde{u}) du = \sigma_Z (-1)^{2p-1} H_{p-1}(\tilde{z}) \phi(\tilde{z}) \qquad (55)$$
$$= -\sigma_z H_{p-1}(\tilde{z}) \phi(\tilde{z}),$$

and then (32) follows by substituting this result into (53).

References

[1] B.C. Levy, Principles of Signal Detection and Parameter Estimation, Springer, 2008.
[2] S.M. Kay, Fundamentals of Statistical Signal Processing. Vol II: Detection Theory, Prentice Hall, Upper Saddle River, NJ, 1998.
[3] A.H. Feiveson, F.C. Delaney, The Distribution and Properties of a Weighted Sum of Chi Squares, NASA Technical Note, no. TN D-4575, 1968.
[4] Z. Wang, P.K. Willett, All-purpose and plug-in power-law detectors for transient signals, IEEE Trans. Signal Process. 49 (11) (2001) 2454–2466.
[5] J. Ma, G. Zhao, Y. Li, Soft combination and detection for cooperative spectrum sensing in cognitive radio networks, IEEE Trans. Wirel. Commun. 7 (11) (2008) 4502–4507.
[6] J. Chen, V.K.N. Lau, Convergence analysis of saddle point problems in time varying wireless systems, IEEE Trans. Signal Process. 60 (1) (2012) 443–452.
[7] V. Banjade, C. Tellambura, H. Jiang, Approximations for performance of energy detector and p-norm detector, IEEE Commun. Lett. 19 (10) (2015) 1678–1681.
[8] P. Berkes, L. Wiskott, Analysis and interpretation of quadratic models of receptive fields, Nat. Protoc. 2 (2) (2007) 400–407.
[9] A. Schlösser, Pricing and Risk Management of Synthetic CDOs, Springer, 2011.
[10] D. Egea-Roca, G. Seco-Granados, J.A. López-Salcedo, Signal-level integrity and metrics based on the application of quickest detection theory to multipath detection, in: Proc. ION GNSS+, 2015, pp. 2926–2938.
[11] C. Stepniak, A representation of nonhomogeneous quadratic forms with application to the least squares solution, Math. Probl. Eng. 2011 (2011) 1–5.
[12] M. Irsigler, Multipath Propagation, Mitigation and Monitoring in the Light of Galileo and the Modernized GPS, PhD Thesis, Universität der Bundeswehr Munchen, 2008.
[13] M. Sahmoudi, M.G. Amin, Robust tracking of weak GPS signals in multipath and jamming environments, Signal Process. 89 (2009) 1320–1330.
[14] K.D. Wesson, J.N. Gross, T.E. Humphreys, B.L. Evans, GNSS signal authentication via power and distortion monitoring, IEEE Trans. Aerosp. Electron. Syst. (2017).
[15] L. Zhao, M.G. Amin, A.R. Lindsey, GPS antijam via subspace projection: a performance analysis for FM interference in the C/A code, Digit. Signal Process. 12 (2–3) (2002) 175–192.
[16] M.G. Kendall, S. Alan, The Advanced Theory of Statistics, 4th ed., Macmillan, 1977.
[17] O. Barndorff-Nielsen, D.R. Cox, Edgeworth and saddle-point approximations with statistical applications, J. R. Stat. Soc. B 41 (3) (1979) 279–312.
[18] A. Freiman, M. Pinchas, A maximum entropy inspired model for the convolutional noise PDF, Digit. Signal Process. 39 (April 2015) 35–49.
[19] A. Papoulis, S.U. Pillai, Probability, Random Variables, and Stochastic Processes, 4th ed., McGraw–Hill, New York, 2002.
[20] D.W. Bolton, The multinomial theorem, Math. Gaz. 52 (382) (1968) 336–342.
[21] B. Guépié, L. Fillatre, I. Nikiforov, Sequential detection of transient changes, Seq. Anal. 31 (4) (2012) 528–547.
[22] A.M. Zoubir, M. Viberg, R. Chellappa, S. Theodoridis, Array and Statistical Signal Processing, vol. 3, Academic Press, 2014.
[23] D. Egea-Roca, G. Seco-Granados, J.A. López-Salcedo, H.V. Poor, A finite moving average test for transient change detection in GNSS signal strength monitoring, in: Proc. IEEE Statistical Signal Processing Workshop (SSP), 2016, pp. 1–5.
[24] H. Cramér, Mathematical Methods of Statistics, vol. 9, Princeton University Press, 1999.
[25] S. Blinnikov, R. Moessner, Expansions for nearly Gaussian distributions, Astron. Astrophys. Suppl. Ser. 130 (1) (1998) 193–205.
[26] E.J. Gumbel, Statistics of Extremes, Courier Corporation, 2004.
[27] N.G. Ferrara, M.J. Pasnikowski, S. Sánchez-Naranjo, F. González, R. Ramos-Pollán, G. Seco-Granados, J.A. López-Salcedo, D. Egea-Roca, M. Solé, M. Toledo, E.S. Lohan, Combined architecture enhancing multi-dimensional signal quality in GNSS receivers, in: Inside GNSS, March/April 2016, pp. 54–62.
[28] A. Pirsiavash, A. Broumandan, G. Lachapelle, Characterization of signal quality monitoring techniques for multipath detection in GNSS applications, Sensors 17 (7) (2017) 1579.
[29] M.T. Gamba, M.D. Truong, B. Motella, E. Falletti, T.H. Ta, Hypothesis testing methods to detect spoofing attacks: a test against the TEXBAT datasets, GPS Solut. 21 (2) (2017) 577–589.
[30] R. Loh, J.P. Fernow, Integrity monitoring requirements for FAAs GPS Wide-Area Augmentation System (WAAS), in: Proc. IEEE Position Location and Navigation Symposium (PLANS), 1994, pp. 629–636.
[31] T.E. Humphreys, J.A. Bhatti, D.P. Shepard, K.D. Wesson, The Texas spoofing test battery: toward a standard for evaluating GPS signal authentication techniques, in: Proc. of the ION GNSS Meeting, 2012.
[32] J.A. López-Salcedo, J.M. Parro-Jiménez, G. Seco-Granados, Multipath detection metrics and attenuation analysis using a GPS snapshot receiver in harsh environments, in: Proc. European Conference on Antennas and Propagation (EuCAP), 2009, pp. 3692–3696.
[33] G. Seco-Granados, J.A. López-Salcedo, D. Jiménez-Baños, G. López-Risueño, Challenges in indoor global navigation satellite systems: unveiling its core features in signal processing, IEEE Signal Process. Mag. 29 (2) (2012) 108–131.
[34] D. Egea-Roca, G. Seco-Granados, J.A. López-Salcedo, On the use of quickest detection theory for signal integrity monitoring in single-antenna GNSS receivers, in: Prof. International Conference on Localization and GNSS (ICL-GNSS), 2015, pp. 1–6.
[35] T.W. Anderson, On the distribution of the two-sample Cramér–von Mises criterion, Ann. Math. Stat. 33 (3) (1962) 1148–1159.
[36] J. Williams, Evaluating user simulations with the Cramér–von Mises divergence, Speech Commun. 50 (2008) 829–846.

Daniel Egea-Roca received the M.Sc. and Ph.D. degrees in electrical engineering from Universitat Autònoma de Barcelona (UAB), Bellaterra, Barcelona, Spain, in 2012 and 2017, respectively. From December 2012 to January 2015, he was involved in the iGNSSrx Project funded by the European Commission. From June to September 2015, and April to June 2016, he was visiting Princeton University, USA. From July to September 2016, he was visiting Hanyang University, South Korea. In 2017, he joined the Department of Telecommunications and Systems Engineering, UAB as a Postdoc Researcher to be involved in the FANTASTIC Project funded by the European GNSS Agency. His research interests include the area of signal processing and its application in threat detection and integrity techniques for GNSS receivers.

Gonzalo Seco-Granados received the Ph.D. degree in telecommunications engineering from Universitat Politècnica de Catalunya, Barcelona, Spain, and the MBA degree from IESE Business School, Madrid, Spain, in 2000 and 2002, respectively. From 2002 to 2005, he was a member of the European Space Agency, involved in the design of the Galileo System. Since 2006, he has been an Associate Professor with the Department of Telecommunications and Systems Engineering, Universitat Autònoma de Barcelona, Spain, and has served as the Vice Dean of the Engineering School since 2011. He has been a Principal Investigator of more than 25 research projects. In 2015, he was a Fulbright Visiting Professor with the University of California at Irvine, CA, USA. His research interests include the design of signals and reception techniques for satellite and terrestrial localization systems, multiantenna receivers, and positioning with 5G technologies. He was a recipient of the 2013 ICREA Academia Award.

José A. López-Salcedo received the M.Sc. and Ph.D. degrees in telecommunication engineering from the Universitat Politècnica de Catalunya, Barcelona, Spain, in 2001 and 2007, respectively. In 2006, he joined the Department of Telecommunications and Systems Engineering, Universitat Autònoma de Barcelona, Spain, where he has been an Associate Professor since 2013. He has been the Principal Investigator of more than 15 research projects, most of them funded by the European Space Agency. He has held several visiting appointments at the University of Illinois Urbana-Champaign, the University of California, Irvine, and the European Commission, Joint Research Centre. His research interests include the field of signal processing for communications and navigation, with emphasis on the combination of GNSS and 5G technologies for accurate and secure positioning.